Soft Matter

PAPER

Cite this: *Soft Matter*, 2021, **17**, 9514

Tunable coffee-ring formation of halloysite nanotubes by evaporating sessile drops†

Hongzhong Liu, Yao Wang, Yumin Luo, Min Guo, Yue Feng and Mingxian Liu *

Received 7th August 2021,
Accepted 18th September 2021

DOI: 10.1039/d1sm01150b

rsc.li/soft-matter-journal

Halloysite nanotubes (HNTs) are one-dimensional clay nanomaterials with a length of 200–1000 nm and a diameter of ~50 nm. Understanding the self-assembly behavior of such unique nanoparticles is important to develop their applications in functional devices. In this study, the "coffee-ring" patterns of HNTs are investigated which are formed by evaporation of the sessile droplets of HNT aqueous dispersion on different substrates. The coffee-ring pattern with various dimensions was characterized using a polarizing microscope (POM), a scanning electron microscope (SEM), and a 3D optical profilometer. The diameter, height, and area of the coffee-ring patterns depend on the concentration of HNT dispersion, the droplet volume, and surface wettability. POM and SEM results suggested that the nanotubes were highly ordered in the edge and the middle of the coffee-ring. The coffee-ring effect of HNTs could be suppressed by increasing the evaporation temperature of substrates or adding polymer additives. In addition, multiple-ring patterns consistent with protein rings surrounding HNT rings were formed, which can be utilized to detect the presence of proteins in biological samples. This work illustrated the relationship between the formation of coffee-ring patterns and the experimental conditions, which provided an additional research chance and allowed application development for HNTs using the liquid droplet self-assembly.

1. Introduction

Evaporation of liquid droplets containing non-volatile solutes or nanoparticles on flat substrates always leaves behind ring-like solid stains, which are called 'coffee-rings'.[1,2] This phenomenon is attributed to the fact that as the volatile solvent evaporates, pinning of the three-phase contact line gives rise to capillary flows that transport non-volatile solutes or nanoparticles to the contact line. The coffee-ring effect dominates many industrial manufacturing processes involving evaporation, such as inkjet printing, biochemical analysis, and micro-manufacturing of patterned structures.[3,4] On the one hand, formation of coffee-ring patterns can be exploited as a method to concentrate the solutes in the solution for analysis and detection.[5] Evaporation of the solvent into a ring-like pattern can increase the analyte concentration making the interfacial reactions more probable. On the other hand, uniform deposition (just like a disk) of nanoparticles without a thick ring is necessary such as in inkjet printing.[6] Therefore, controlling the coffee-ring effect of the related deposit pattern is the key issue, which can be achieved by changing the external factors and formulations. For example, numerous studies have been conducted on the suppression of the coffee-ring effect *via* using electrowetting, high-aspect-ratio particles, rapid evaporation speeds, hydrophobic surfaces as substrates, and addition of surfactants and polymers.[3] Nanoparticles which can form "coffee-ring" patterns by droplet evaporation include polymer colloid particles,[7] DNA,[8] proteins,[9] porphyrin trimers,[10] semiconductor nanoparticles,[11] gold nanoparticles,[12] carbon nanotubes,[13] graphene,[14] and metal–organic frameworks (MOFs).[15] It is very interesting to explore new nanoparticles for understanding the coffee-ring pattern deposition process.

Halloysite nanotubes (HNTs) are natural clay nanotubes with empty lumen and a high aspect ratio. HNTs have a typical outer diameter of 50 nm, while the length of the tubes ranges from 500 to 1500 nm.[16,17] As novel one-dimensional nanomaterials, HNTs show great potential in high-tech areas such as polymer composites, wound healing, drug delivery, cosmetics, and biosensors.[18] For these applications, understanding the assembly behavior of the nanotubes and preparation of ordered HNT micropatterns is essential to optimise the device performance. Our previous work revealed the assembly behavior of HNTs under confined space or external force, and related application of the ordered pattern structure was suggested.[19] The confined space for the assembly of HNTs included cylindrical tubes, sphere-on-flat geometry,[20] and a two-plate configuration (vertical or flat).[21,22] It is interesting that HNTs can assemble into ordered stripe patterns with the alignment of the tubes on these stripes. These assembled structures can be used to guide cell growth and capture of tumor cells from blood samples. The nanotubes can also be well aligned

Department of Materials Science and Engineering, Jinan University, Guangzhou 510632, China. E-mail: liumx@jnu.edu.cn

† Electronic supplementary information (ESI) available. See DOI: 10.1039/d1sm01150b

with shear forces supplied by commercial brushes.[23] The coffee-ring effect of poly(styrene sulfonate) modified HNTs was firstly reported by Zhao *et al.*, and the factors such as particle concentration, tubes' length and charge, pH and ionic strength, and evaporation temperature which affect the alignment of the tubes were investigated.[24] However, the prepared so-called coffee-ring was actually an intermediate pattern of an ordered ring and uneven deposition of HNTs, and the suppression of the coffee-ring effect of HNTs was not investigated.

In this study, a clear and round ring of HNTs by the evaporation-induced self-assembly of their sessile droplets was investigated. The width, diameter, height, and area of the coffee-ring pattern are dependent on the concentration and volume of HNT droplets. The tubes are organized in a highly ordered manner in the coffee-ring. The formation of coffee-rings can be suppressed by increasing the substrate temperature or adding polymers. Various ordered patterns of HNTs can be obtained by changing the droplet shapes. In addition, multiple-ring patterns consistent with protein rings surrounding HNT rings were formed, which can be used to sort particles of different sizes and detect the presence of proteins during drying. This work illustrated the relationship between the coffee-ring patterns and the experimental conditions, which provided additional research chance and application of HNTs using a liquid droplet self-assembly process.

2. Experiments and characterization

2.1. Materials and reagents

Halloysite nanotubes (HNTs) were obtained from Guangzhou Runwo Materials Technology Co., Ltd, China. Polyvinyl pyrrolidone (PVP) (K30) was purchased from Suzhou Meilun Biotechnology Co., Ltd, China. Bovine serum albumin (BSA) was purchased from Guangzhou Sijia Biotechnology Co. Ltd, China. Glass slides (75×25 mm^2) were purchased from Citotest Scientific Co. Ltd, China. Sheets of polystyrene (PS), polymethyl methacrylate (PMMA), and silicified glass were obtained from the local market. Other chemicals used in this study were of analytical grade and used as received. Ultrapure DI water was purified by deionization and filtration with a Millipore purification apparatus (resistivity >18.2 MΩ cm).

2.2. Preparation of HNT dispersion

Different HNT dispersions were prepared using an ultrasonic treatment method. Before preparation of the dispersion, HNTs were purified to remove quartz and alunite. The zeta potential of the used HNTs was −20.2 mV, and no surfactant such as polystyrene sulfonate sodium was added during the preparation of the dispersion. In a typical procedure, 0.2, 0.4, 0.8, and 1.6 wt% HNT dispersions were obtained by dispersing HNTs *via* ultrasonication (40 kHz) in 50 mL of ultrapure water for 10 min.

2.3. Preparation of coffee-ring patterns

Typically, 10 μL HNT dispersions with different concentrations were dropped onto the surface of glass slide substrates. The water of the droplets evaporated on a temperature controlled hot stage. HNT coffee-ring patterns were formed during the evaporation induced self-assembly process. The influence of the HNT concentration, droplet volume, substrate type, evaporation temperature, and additive (PVP) on the formation of coffee-ring patterns was investigated. The concentrations were 0.2, 0.4, 0.8, and 1.6 wt%, while the droplet volumes were 2.5, 5, 10, and 50 μL. The substrates were commercial glass slides, PS, PMMA, and silicified glass sheets. The evaporation temperature was set as 25, 35, 50, 75, and 110 °C to investigate the effect of the formation of coffee-ring patterns. PVP concentrations were 0.1, 0.2, and 0.4 wt% relative to the total dispersion weight.

2.4. Characterization

2.4.1. Field emission scanning electron microscopy (FE-SEM). The geometric morphologies of HNTs and coffee-ring patterns were observed using an FE-SEM (ULTRA55, Carl Zeiss Jena Co. Ltd., Germany) at 5 kV. Before FE-SEM observation, the samples were sputter-coated with gold films with a thickness of 5 nm.

2.4.2. Polarized optical micrography (POM). The HNT coffee-ring pattern was formed on a glass slide and photographed by using a polarized optical microscope (BX51, Olympus Corporation, Japan).

2.4.3. Stereo microscope. The coffee-ring pattern was photographed by using the Stereo microscope (SteREO Discovery V 20., ZEISS, Germany).

2.4.4. Contact angle tester. A contact angle tester ((DSA100, Kruss Ltd, Germany) was used to test the water contact angles (WCAs) at room temperature. The measurement of water contact angles was performed immediately after the release of water droplets on the surface of substrates. The volume of the water droplet was 10.0 ± 0.5 μL. At least five measurements were taken for each substrate. The contact angles of the HNT/BSA mixture were tested in the same way.

2.4.5. 3D morphology. The surface morphology and profiles of HNT coffee-ring patterns were analyzed using a 3D optical profilometer (UP-DUAL MODE, Rtec Engineering Ltd., USA) with a magnification of 20×. The line profiles were obtained by analyzing the 3D topography using the Gwyddion analysis software.

2.4.6. Infrared thermal imager. An infrared thermal imager (TiS 55, Fluke Electronic Instrument Ltd., USA) was used to take thermal imaging pictures of HNT droplets forming coffee-rings at different temperatures. The SmartView software was used to measure the temperature at different positions of the droplets.

2.4.7. Analysis of the orientation degree. According to SEM images of the samples, the orientation characteristics were extracted using the image processing tools and programs of MATLAB. Based on the angle between the inscribed ellipse major axis and x-axis in the reflective area of HNTs, the frequency of the sample orientation was obtained.

2.4.8. Analysis of the width and diameter of coffee-rings. The images of coffee-ring patterns were photographed using a polarized optical microscope. The standard length was set up by measuring the length which was known. The images were used to measure the width and diameter of coffee-rings using ImageJ.

3. Results and discussion

3.1. The formation process of HNT coffee-ring patterns

The experimental material is HNTs, which are a typical one-dimensional tubular nanomaterial with unique morphology (Fig. S1, ESI†). According to previous studies,[22] the formation of the coffee-ring patterns requires three conditions: (i) the droplet contains non-volatile particles; (ii) the contact line of the droplet can be pinned on the substrate; and (iii) the droplet evaporates with time and the Marangoni flow should be suppressed. The HNTs contained in the droplets are non-volatile nanoparticles and they meet condition (i). As the evaporation time elapsed, the contact angle and volume of the droplet decreased linearly. The contact line between the droplet and the substrate was still pinned so that the contact radius remained constant (Fig. 1A), which met conditions (ii) and (iii). As a result, HNT droplets formed the coffee-ring pattern finally during the faster evaporation process (Fig. 1B). The changes of the contact angle and droplet volume are shown in Fig. 1C. The pinned three-phase contact line led to the capillary flow inside the droplet to move to the edge to supplement water. In this process, the nanotubes moved to the edge with the capillary flow of the dispersion. The reason for the capillary flow moving to the edge was that the volume of the droplet became smaller due to the evaporation of water. If there was not any supplement of water, the radius of the droplet would shrink. The contact line was pinned and the radius could not be reduced, which forced the capillary flow to move outward and transport the water to the three-phase line position.

In order to further explore the formation mechanism of the HNT coffee-ring pattern, a polarizing microscope (POM) was used to record the ring formation process at different times.

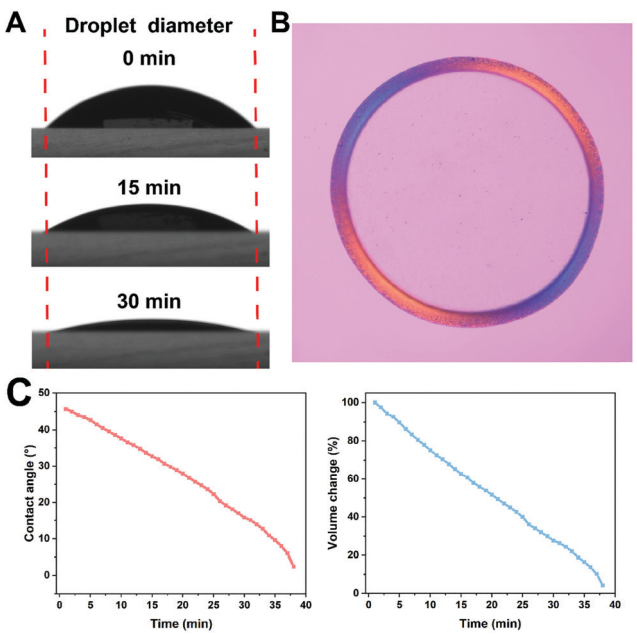

Fig. 1 Photos of HNT droplet at different evaporation times (A); polarizing microscopy image of the HNT coffee-ring pattern (B); and contact angle and volume change curves of the HNT droplet with evaporation time (C).

It can be seen from Fig. 2A that the nanotubes were uniformly dispersed in the water at the beginning. As time went by, the water gradually evaporated and the nanotubes accumulated at the three-phase line. The nematic phase starts to appear due to the increased nanotube concentration and the alignment of the tubes at the pinned line. Then the coffee-ring pattern formed by evaporation of the HNT dispersions gradually thickened and the yellow area became larger and larger. Finally, the water completely evaporated and the coffee-ring composed of aligned HNTs was completely formed. The change of the droplet edge (black) to ring (yellow) confirmed the process of ordered arrangement of HNTs.

To be precise, the evaporation-induced self-assembly process of the HNT forming coffee-ring pattern can be divided into five different stages: t1–t5 (Fig. 2B). At the t1 stage, HNTs were uniformly distributed in the droplets and showed isotropy. In the t2 stage, due to the evaporation of water and the pinning of the three-phase line, the HNTs inside the droplet moved to the edge with the capillary flow and the HNT content in the edge zone increased, which promoted the orientation of HNTs parallel to the edge and the formation of the liquid crystal phase. The reason for the orientation was that HNTs are anisotropic nanoparticles. When one end of the nanotube was in contact with the pinning line, the capillary flow would apply the torque at the other end to make it parallel to the contact line.[25] From the t2 to t3 stage, the capillary flow rate was stable and the coffee-ring uniformly formed while the nanotubes were further aligned. During the transition from the t4 to t5 stage, the velocity of capillary flow increased suddenly, which caused the HNTs to rush to the edge. Finally, the coffee-ring formed until the water completely dried. The formation process of the coffee-ring pattern by drying HNT droplets was recorded as a video (Video S1, ESI†). Fig. 2C and D show the normalized ring width and velocity as a function of evaporation time. The width is the maximum ring width (the ring width obtained after evaporation) that is normalized and the velocity speed is normalized ring width/drying time. The drying rate of the ring from 0 to 16 min was relatively average, which showed a slow increasing trend. When the drying time was from 18 to 22 min, the speed of forming the ring suddenly increased. Fig. 2C shows that about 35% of the coffee-ring width was formed in the last 4 minutes, which indicated that during the last 18% of the total drying time, more HNTs formed coffee-rings. The sudden increase in particle density at the edge of the droplet could be regarded as "edge effect", which hindered the migration of HNTs and affected their orientation.[26] Therefore, the nanotubes which reached the edge in the final stage of evaporation precipitated in a relatively disordered arrangement as the water completely evaporated.

Considering the aspect ratio of the particles alone, it is generally more difficult for anisotropic particles to form a coffee-ring than isotropic particles.[27] However, the interactions between particles would also affect the self-assembly behavior. HNTs repelled each other due to the high surface negative potentials and were well dispersible in the dispersion, and the nanotubes could be transported to the edges of the droplet and

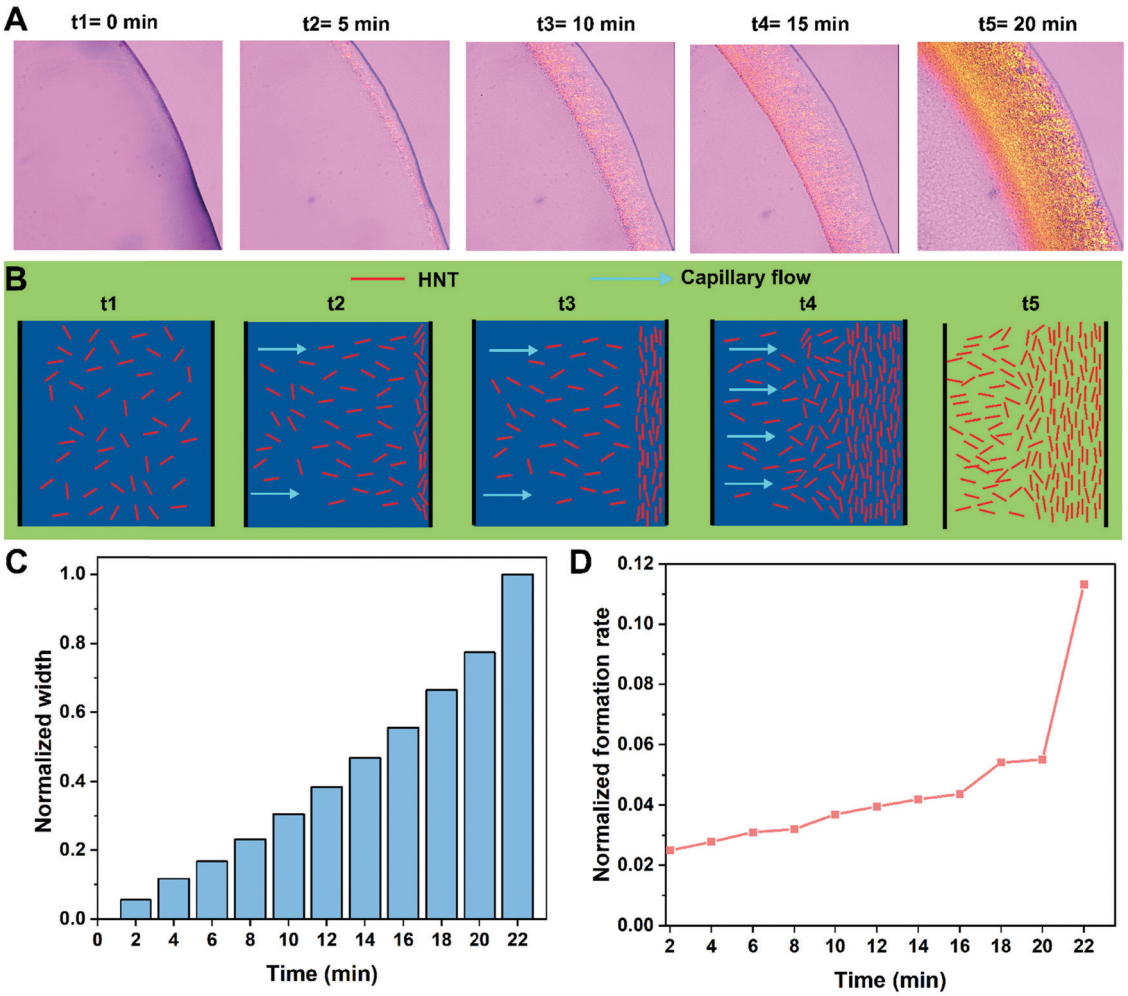

Fig. 2 POM image (A) and schematic diagram (B) showing the HNT coffee-ring formation process; curves of normalized ring width (C) and formation speed (D) of the HNT coffee-ring with time.

form a coffee-ring.[28–30] A high pH value resulted in an increased zeta potential of the tubes, which was beneficial to the formation of the ordered structure of the coffee-ring. Also, the formation of the coffee-ring is mainly dependent on the interactions between the solute and the substrate (pinning of the contact line). It was found that the increased length and aspect ratio of HNTs resulted in better organization in the coffee-ring structure since the excluded volume interactions between the tubes in a given volume are dependent on their length. As the length increases, the arrangement of HNTs in the coffee-ring will become more orderly because the entropy of the nematic phase is maximized with the long-range orientation of the nanotubes,[24] while the short HNTs tend to be arranged disorderly in the coffee-ring pattern.

The POM image of the coffee-ring pattern of HNTs showed obvious birefringence (Fig. 3A), which suggests that the nanotubes in the coffee-ring were in an ordered structure. Subsequently, scanning electron microscopy (SEM) was utilized to study its microstructure. It can be seen from Fig. 3A that HNTs present different orientation structures at different positions of the ring. The nanotubes at the edge of the ring showed partial order. The outer HNTs were perpendicular to the edge, while the inner nanotubes became gradually parallel to the edge. This position could be considered to be that the nanotubes near the contact line had not yet reached the pinning concentration and contracted slightly inwardly during the initial evaporation. The outermost HNTs were fixed when they were too late to align. The nanotubes in the inner part of the edge were located in the three-phase line, and they had enough time to be oriented parallel to the edge. The nanotubes in the middle of the ring also had a good alignment effect. The speed of the capillary flow was slow and uniform, which was beneficial for the orientation of HNTs. Therefore, HNTs were parallel to the edges and have the highest degree of orientation (Fig. 3B). The inner edge of the ring was in the final stage of the drying process. As mentioned above, the capillary flow rate increased rapidly during this period of time, the concentration of HNTs suddenly increased and the water quickly evaporated, which affected their ordered arrangement due to the high viscosity and the short time for moving.[7] Therefore, this part of the nanotubes retained the state of moving with the capillary flow to the edge, and the overall distribution of the nanotubes

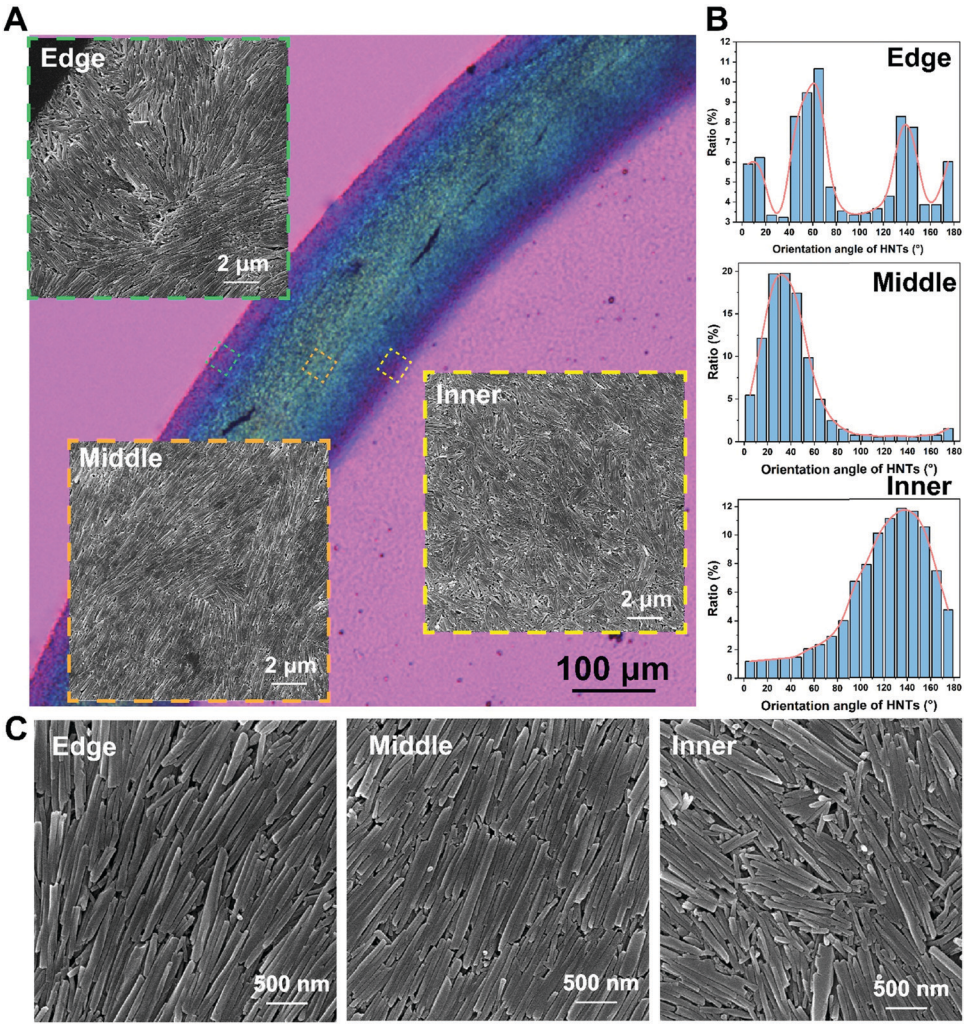

Fig. 3 POM and SEM images of the HNT coffee-ring (A); corresponding orientation statistics (B) and corresponding enlarged SEM (C).

was perpendicular to the edge. Fig. 3C shows the enlarged SEM images of HNTs at different positions, which more clearly show the different arrangements and distributions of HNTs at the edge, middle, and interior. These results are highly consistent with the previous study on the coffee-ring effect of HNTs.[24]

3.2. Effect of HNT droplet concentration and volume on the coffee-ring pattern

In the following sections, we investigated the factors which affect the formation of the coffee-ring pattern of HNTs. Fig. 4A and Fig. S2 (ESI†) show that HNT droplets at concentrations from 0.2 to 1.6 wt% could form coffee-ring patterns. The patterns show obvious birefringence under polarized light, which indicates that there were ordered nanotubes in the coffee-rings at different concentrations. Increasing the concentration of HNTs, the width of the coffee-ring increased gradually, but the diameter remains basically unchanged (Fig. 4B and C). The mathematical statistical relationship between the ring width and HNT concentration is shown in Fig. 4B. Taking the droplet volume of 2.5 μL as an example, when the concentration increased from 0.2 wt% to 1.6 wt%, the width of the ring increased from 88.4 μm to 235.9 μm. The water was completely evaporated during this process, and the coffee-ring was entirely composed of HNTs. When the concentration of HNTs increased, the same volume of dispersion contained more HNTs and more nanotubes formed a thicker ring width on the glass slide.

In addition, the concentration of HNT droplets also affected the height of the coffee-ring pattern. Also, we take the 2.5 μL droplet volume as an example, the height of the coffee-ring increased when the concentration of HNTs increased (Fig. 5A and B). The height of the coffee-ring changes from 11.5 μm to 32.8 μm while the diameter remains at about 2700 μm, which is in agreement with the results observed in the POM result above. The coffee-ring was formed by evaporation of HNT droplets. The diameters of the coffee-rings were basically the same because the spreading ability of HNT dispersions with different concentrations on the glass slides is similar and the droplets are similar in size. The volume of the coffee-ring pattern could be calculated by combining the ring width, diameter and height (Fig. 5C). The result showed that the volume of the coffee-ring increased exponentially with the concentration, which indicated that most of the HNTs contained

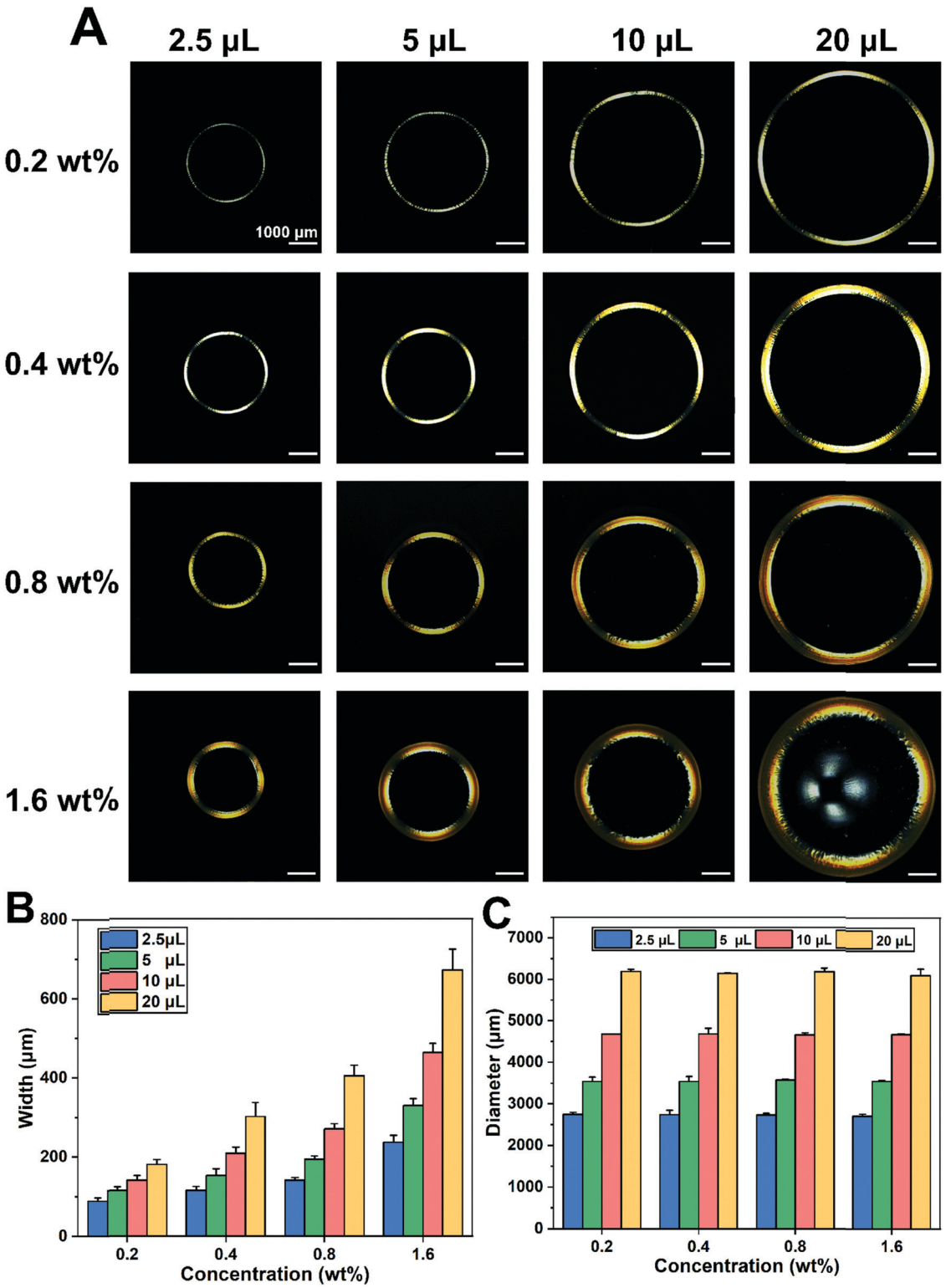

Fig. 4 The effect of HNT concentration and droplet volume on coffee-ring patterns: POM images (A); corresponding ring width (B) and diameter (C).

in the droplets were concentrated on the edge of the droplet to form the coffee-ring. Therefore, the size of the coffee-ring pattern could be controlled by adjusting the concentration of HNT droplets.

In order to examine the effect of droplet volume on coffee-rings, different volumes of HNT droplets were used to form coffee-ring patterns. The volume of the droplet could significantly affect the width and diameter of the coffee-ring (Fig. 6A)

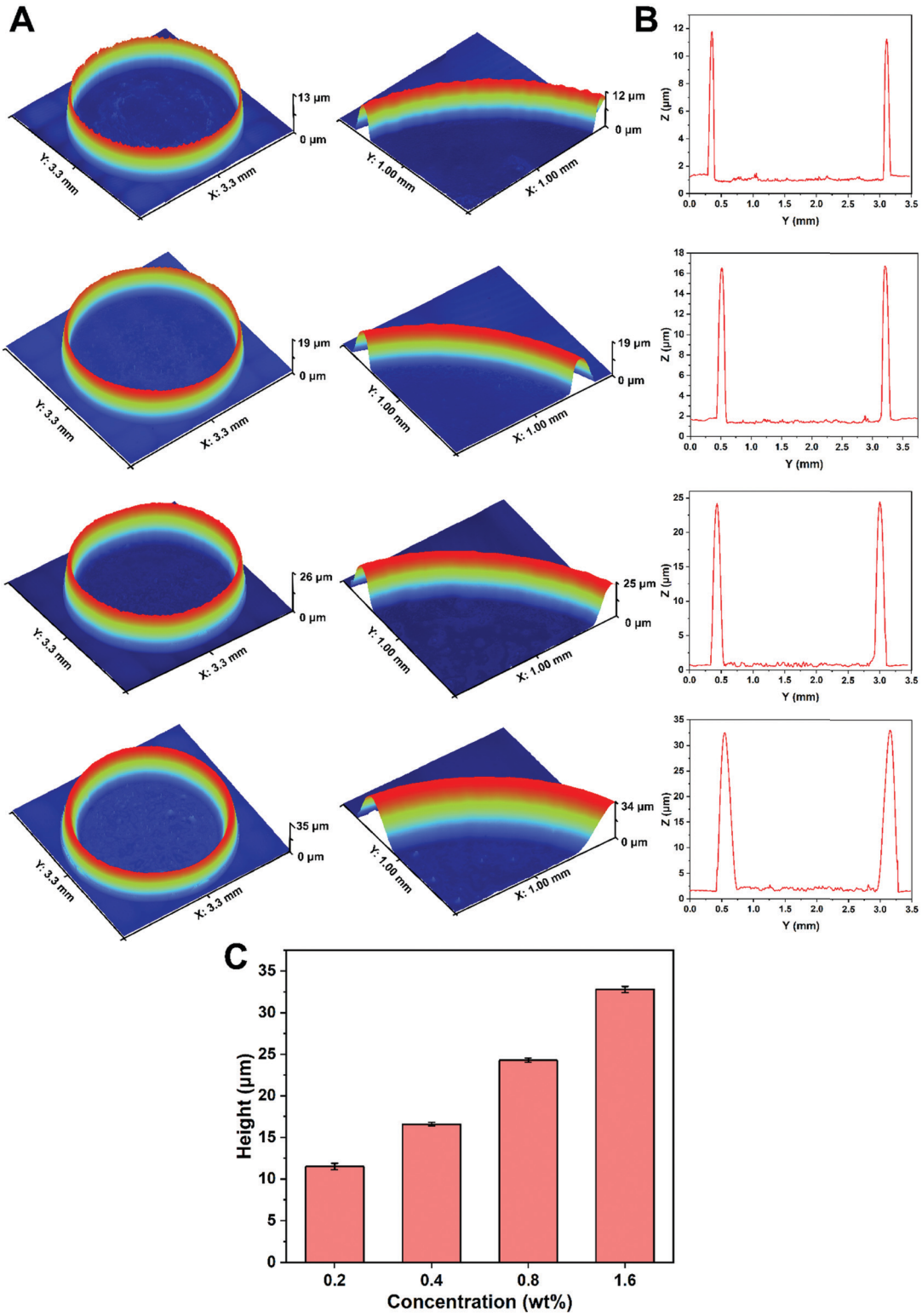

Fig. 5 3D topography images (A), thickness curves (B), and height statistics (C) of the coffee-ring patterns formed by the different concentrations of HNT droplets.

for all samples at different concentrations. Taking the dispersion with 0.4 wt% concentration as an example, the ring width increased from 114.9 μm to 300.7 μm and the diameter increased from 2737.8 μm to 6145.6 μm when the droplet volume increased from 2.5 μL to 20 μL. Both of them increased with the increase of the droplet volume. Different from the

increase in the concentration of HNTs of liquid droplets, increasing the volume of dispersion not only increases the content of HNTs, but also increases the volume of the formed droplets. Due to the similar spreading ability of droplets, the area on the substrate will also increase, so the diameter of the coffee-ring increased with the increase of droplet volume. In addition, the volume of droplets also affects the height of the coffee-ring pattern. The height of the coffee-ring increases with the increase of the droplet concentration (Fig. 6B). From the height statistics graph, the height of the coffee-ring increased from 16.6 μm to 30.2 μm. Compared with the effects of concentration and volume on the height of the coffee-ring, it was found that the height affected by concentration can increase by 3 times while the height affected by volume only increased by 2 times when the HNT content both increased by 4 times. The reason is perhaps that the increase of HNT content by increasing the droplet volume would not only increase the ring width, but also increase the diameter, so that the area of the whole coffee-ring would become larger. For maintaining the same degree of increasing the ring width by increasing the concentration, the height of the coffee-ring could only be reduced. It can be known by calculation that the volume of the formed coffee-ring increased in multiples to a similar degree to the increase in the droplet volume. So, the width, diameter and height of the coffee-ring pattern could be controlled by adjusting the volume of HNT droplets. When one changed the droplet shape by using three/four drops or dropping a smaller one after drying a bigger ring, different HNT patterns with a merged structure can be formed on the substrates (Fig. S3 and S4, ESI†).

3.3. Effect of the surface wettability on HNT coffee-ring patterns

The difference in the wettability of the substrate surface would cause the HNT dispersion to form droplets with different contact angles which further affect the formation of coffee-rings. In order to verify the influence of substrate wettability on the formation of coffee-rings, the HNT droplets were dropped on four different substrates. 10 μL HNT dispersion would form droplets with different contact angles (CA) on different substrates: adhesive glass slide (CA= 45.0 ± 3°), PS (CA = 58.4 ± 3.2°), PMMA (CA = 71.1 ± 3.8°) and siliconized glass (CA = 103.8 ± 2.3°). Comparing substrates with different hydrophobic properties using stereomicroscopy images (Fig. 7), it was noticed that the height of the droplets increased and the contact diameter decreased when the contact angle increased, which led to smaller coffee-ring patterns. The size and brightness of the coffee-rings formed by PS and PMMA with similar contact angles were similar. A similar brightness indicated that the density of HNTs in the ring was similar. It is worth mentioning that when the HNT droplets evaporate on the siliconized glass, the three-phase contact line did not pin to the substrate at the initial stage until the droplet volume and contact area were reduced to a certain extent. This may be due to the strong hydrophobicity of siliconized glass which had weak interactions with HNTs. The pinning was achieved when the HNT concentration increased by evaporating water in the droplet. The coffee-ring which formed on the siliconized glass showed the highest density of the nanotubes compared with the other three substrates as it exhibited the highest brightness (Fig. 7). Therefore, HNT coffee-rings can be controlled by changing the degree of hydrophilicity and hydrophobicity of the substrate.

3.4. Effect of substrate temperature on HNT coffee-ring patterns

The effect of evaporation temperature on the formation of coffee-ring patterns of HNT droplets (1.6 wt%) was explored by changing the substrate temperature. Fig. S5 (ESI†) shows the

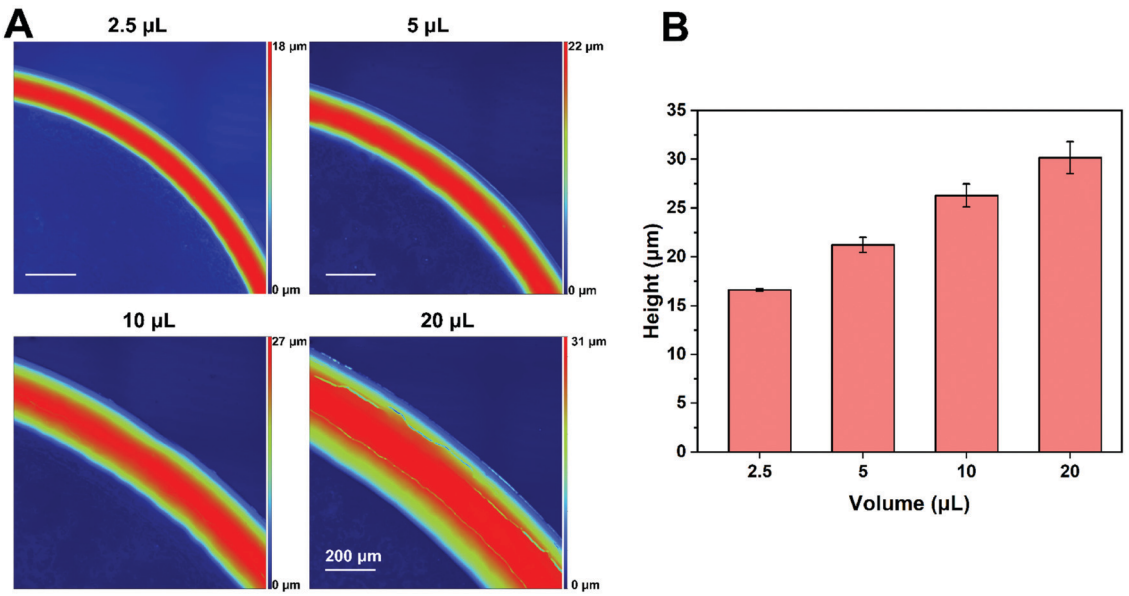

Fig. 6 Topography images (A) and height statistics (B) of the coffee-ring patterns formed by the different volumes of HNT droplets.

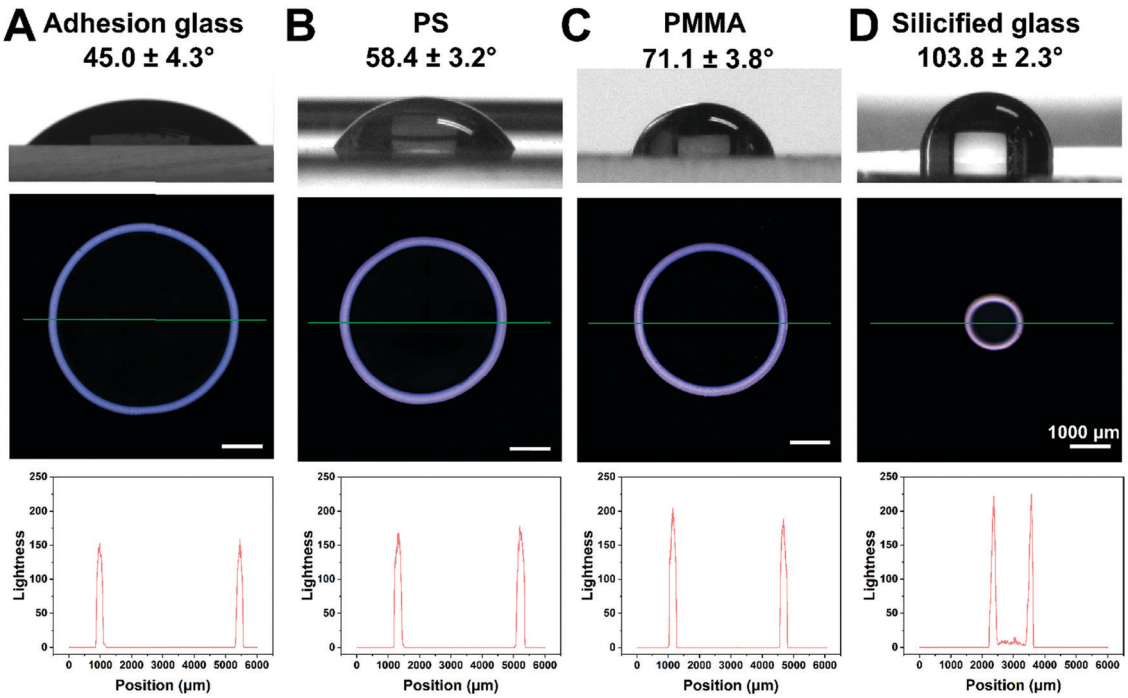

Fig. 7 Coffee-ring patterns of HNT droplets on different wettability substrates: adhesion glass (A); PS (B); PMMA (C); and silicified glass (D). The contact angle images (top) of HNT droplets (10 μL), stereomicroscopy images (middle) and corresponding brightness (bottom).

appearance of the HNT coffee-ring patterns formed at different substrate temperatures with different concentrations. It can be seen by evaluating the evaporation temperature that the coffee-ring pattern transited from a perfect single ring to an intermediate pattern just like an eye shape,[31] and finally a uniform deposition pattern like a disk was obtained. Fig. 8A shows the stereomicroscopy images of HNT droplets forming coffee-rings at different substrate temperatures. The corresponding normalized gray scale transmitted light intensity profiles (G_N) obtained by ImageJ from the microscopy images. Depending on previous studies, this intensity has a good positive correlation with the thickness of the coffee-ring.[32] Combining the microscopy image and the G_N curve, the vast majority of HNTs were concentrated in the coffee-ring at the edge and there was only a very small amount of HNTs in the inner area at 25 °C. The pattern of the coffee-ring was still clear, but the content of HNTs in the inner area had increased with an increase of the substrate temperature. From the G_N curve, it can be seen that the inner gray scale has increased slightly when the substrate temperature increased to 35 °C. The boundary between the coffee-ring and the uniformly deposited HNTs was blurred when the substrate temperature increased to 50 °C. Although the thickness of the inner layer of HNTs was smaller than that of the edge (coffee-ring) from the G_N curve, there was a tendency to deposit from the edge to the center of the pattern. HNTs no longer formed a coffee-ring, but a disc-like pattern at 75 °C. It can be observed that HNTs are basically uniformly deposited throughout the disc except for some gaps in the center.

In order to understand the influence of substrate temperature on the self-assembly of HNTs to form a coffee-ring, an infrared thermal imager was used to capture the temperature distribution of HNT droplets at 35 and 75 °C. At 35 °C, the colors of the various positions of the droplets were similar, and there was no obvious temperature difference with only low temperature at the center of the droplet (Fig. 8B). The color of the droplets was obviously different at 75 °C, which showed 6 different colors: pink, dark blue, sky blue, green, yellow, and orange. This indicated that the droplet has a significant temperature difference at different positions, which showed a trend of increasing temperature from the vertex to the edge. The high substrate temperature results in a speedy evaporation rate for the water and an accelerated drying rate.

In the process of the formation of the coffee-ring by HNT droplets, there were not only the radial capillary flow and the gravity flow from top to bottom, but also a Marangoni flow driven by heat. The Marangoni flow is produced by the difference in surface tension (surface tension gradient). In the same droplet, the surface tension is high in the position with low temperature, and the surface tension is low in the position with high temperature. Therefore, the Marangoni flow will flow from a place with a high temperature to a place with a low temperature.[33] Fig. 8C was used to explain the effect of drying at different substrate temperatures on the formation of coffee-rings by HNT droplets. Since the rate of the Marangoni flow is positively correlated with the temperature difference (ΔT), with a greater temperature difference, the Marangoni flow rate is faster.[34] The coffee-ring was formed because the three-phase line was pinned to the substrate so that the capillary flow transferred the nanotubes radially outward to the contact line. The Marangoni flow moved from the edge to the apex because

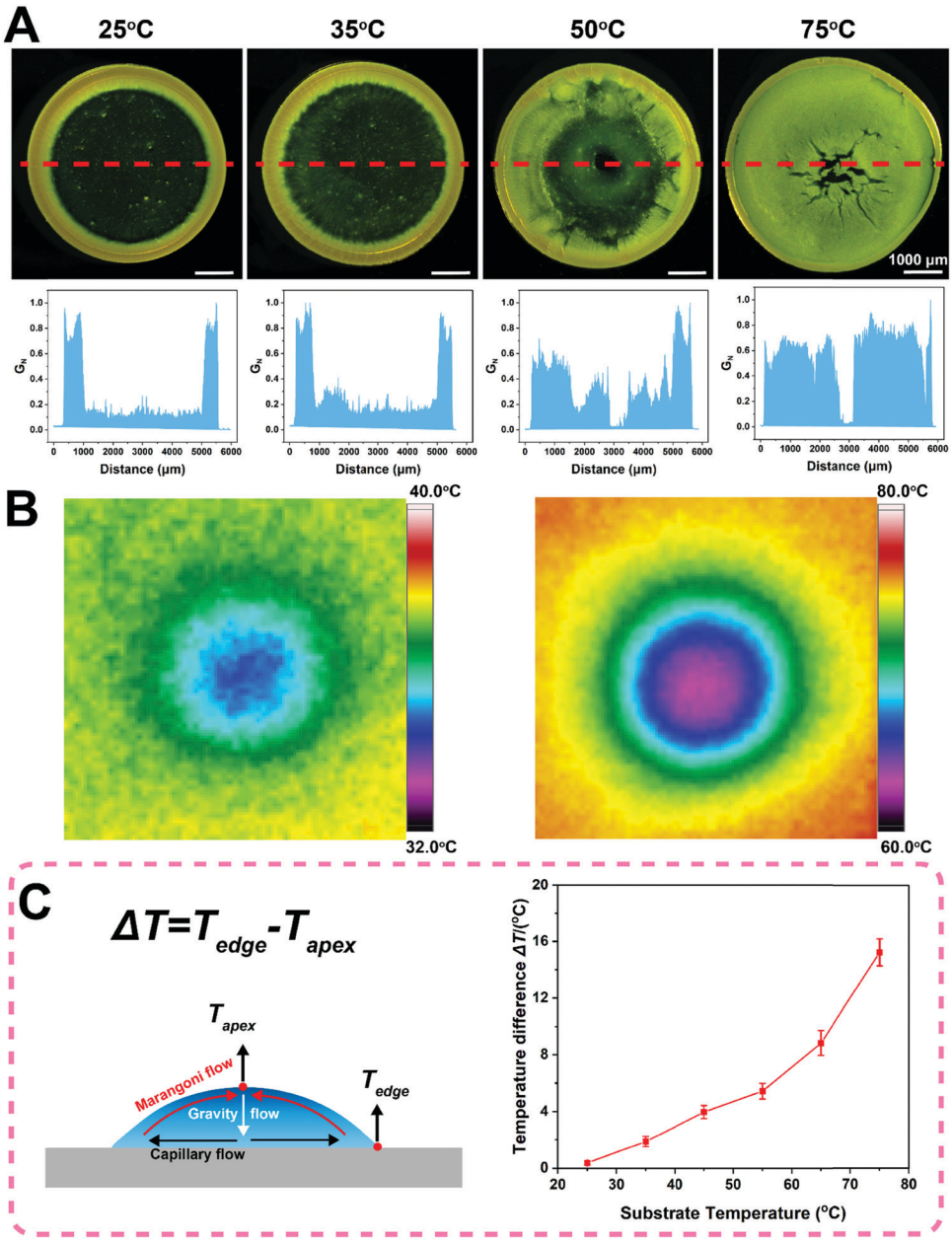

Fig. 8 Microscopy images of the coffee-ring patterns formed by drying HNT droplets at different temperatures and the gray intensity (G_N) curves marked along the dotted lines on the corresponding images (A); thermal imaging photos of HNT droplets at different drying temperatures (B); a schematic diagram of the Marangoni effect in a droplet and the temperature difference curve between the edge and the apex of the droplet at different drying temperatures (C).

the temperature of the apex was lower than that of the edge, and it moves the nanotubes from the edge to the apex at the same time, which reduced the concentration of HNTs at the edge and inhibited the formation of coffee-rings. Fig. 8C was drawn by measuring the temperature difference between the apex and edge of the HNT droplet at different substrate temperatures. It can be found that the higher the substrate temperature, the greater the temperature difference at different positions of the droplet. This suggested that increasing the substrate temperature can increase the Marangoni flow and inhibit the formation of coffee-rings, which is consistent with that shown in Fig. 8A.

3.5. Effect of addition of polymers on HNT coffee-ring patterns

The Marangoni effect caused by the surface tension gradient can not only be merely driven by heat, but also by the addition of surfactants. The nonionic surfactant polyvinylpyrrolidone (PVP) was employed as an example in this work. PVP can be easily dissolved in the HNT aqueous dispersion and has stable physical and chemical properties under normal conditions. Compared with pure HNT dispersion, the contact angle of HNT dispersion after adding PVP was significantly reduced. As the concentration of PVP increased, the contact angle

gradually decreased (Fig. 9A). The contact angle decreased from 45.0° to 27.8° (38%) when the concentration of PVP increased from 0 wt% to 0.4 wt%. Therefore, PVP was demonstrated to be a suitable surfactant, which can effectively reduce the surface tension of HNT dispersion.

Most of the nanotubes were gathered on the coffee-ring, and almost no HNTs exist inside when there was no PVP added. The coffee-ring was still clear, but some HNTs have begun to deposit inside when 0.1 wt% PVP was added. As the concentration of PVP increased, the boundaries of the coffee-ring became blurred. The coffee-rings of 0.2 wt% PVP were almost invisible in the digital photos, but the presence of coffee-rings was still observed in the microscope. When the concentration of PVP reached 0.4 wt%, the presence of coffee-rings could not be observed from digital photos or microscopy pictures. HNTs were uniformly distributed throughout the formed disk. SEM was used to observe the microstructure of the disk formed by the droplets of HNTs with 0.4 wt% PVP (Fig. 9B). The HNTs were evenly distributed on the edge, inside, or center of the disk. Unlike HNTs that form coffee-rings, these HNTs were arranged in random orientations. The reason why the addition of PVP can inhibit the production of coffee-rings is due to the Marangoni flow. HNTs gathered at the edge with the capillary flow to form the coffee-ring when no PVP was added. When PVP was added, the capillary flow moved both HNTs and PVP to the edge. PVP reduced the surface tension at the edge of the droplet, while the surface tension at the top of the droplet which lost the most PVP under the action of gravity flow and capillary flow was the highest. The difference in surface tension produced a Marangoni flow that moved from the edge to the top and it moved the HNTs while transferring PVP.[35] Like the model presented in Fig. 8C, the circulating flow which made the concentration of HNTs uniform at each location inhibited the formation of coffee-rings and made HNTs evenly deposited.

3.6. Effect of different factors on the time for HNT droplets to form coffee-ring patterns

The evaporation time for the HNT droplets to form a coffee-ring is affected by various aspects such as HNT concentration, droplet volume, substrate temperature, and substrate material. Fig. 10 shows the influence of different factors on the time for HNT droplets to form a coffee-ring. The substrate temperature had a significant effect on the evaporation time (Fig. 10A). For example, when the temperature was increased from 25 °C to 110 °C, the drying time decreased from 25 min to 0.8 min which declined as high as 97%. The droplet volume also had an obvious influence on the drying time, but the impact was not as good as the substrate temperature (Fig. 10B). The volume was increased from 2.5 μL to 20 μL (an 8-fold increase) while the drying time was increased from 11 min to 36 min (only 3.5 times increase). This happens because the increase in volume would also increase the spreading area (evaporation area) of the droplets. Although the increase in area was less than the increase in volume, it would also reduce the increase in evaporation time. In conjunction with Fig. 10A and B, it was found that the concentration of HNTs in the droplets will also

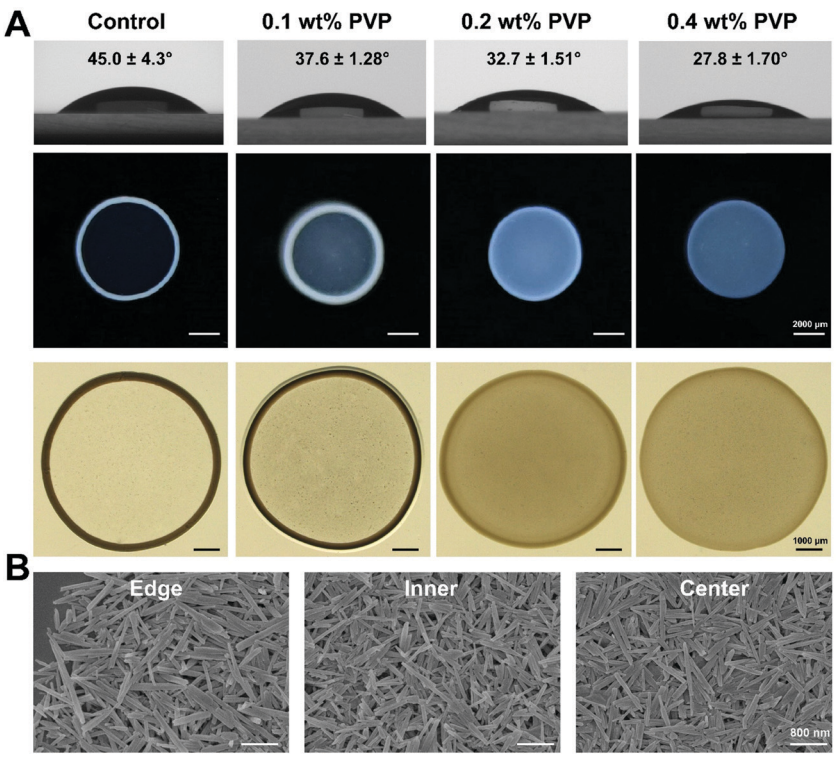

Fig. 9 Photographs of contact angles of HNT dispersions with different concentrations of PVP as well as digital and microscopy pictures after the droplets are dried (A); SEM of the 0.4 wt% PVP and HNT dispersions dried to form discs (B).

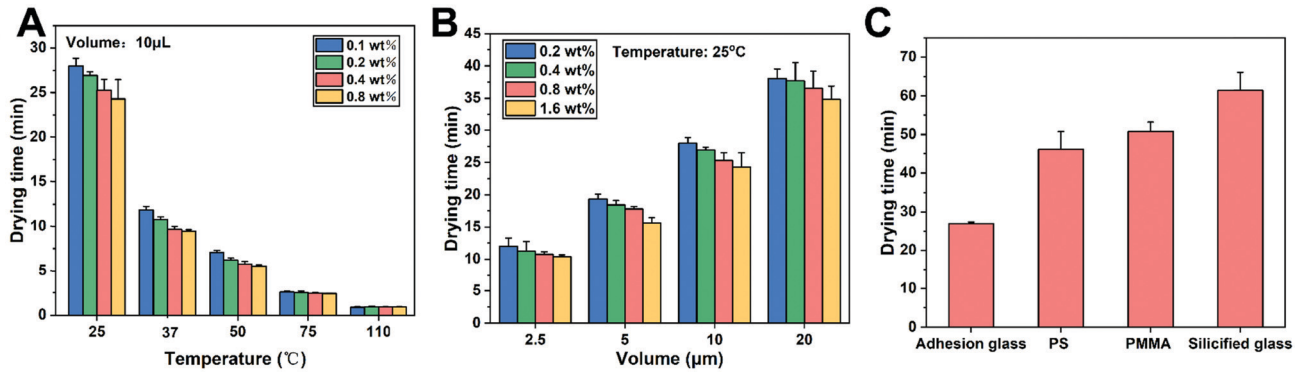

Fig. 10 Effects of different factors on the HNT coffee-ring pattern formation time: substrate temperature (A), droplet volume (B), and substrate material (C).

have a certain effect on the drying time. Under the same conditions, the higher the concentration of the droplets, the shorter the drying time. This may be explained by the fact that when the concentration of the droplet is higher, it contained more HNTs and a lower amount of water. In the drying process, a small part of the water in the droplets was absorbed by HNTs except for evaporation into the air and the droplets containing more HNTs would absorb more water, which shortened the drying time. Comparing the substrate temperature and the droplet volume, the droplet concentration had a little significant effect on the drying time.

A 10 μL drop of HNTs was employed as an example and the evaporation time was recorded on different substrates (Fig. 10C). It can be seen that the drying time on the adhered glass slide was the shortest, while the time on the siliconized glass was the longest. The drying time of PS and PMMA was in the middle and similar. This can be attributed to their different contact angles as shown in Fig. 7A. The different wettability of the substrate resulted in different areas of the droplets spreading on the surface. For the same volume, the evaporation area of the droplets on the adhesion glass slide was the largest, followed by

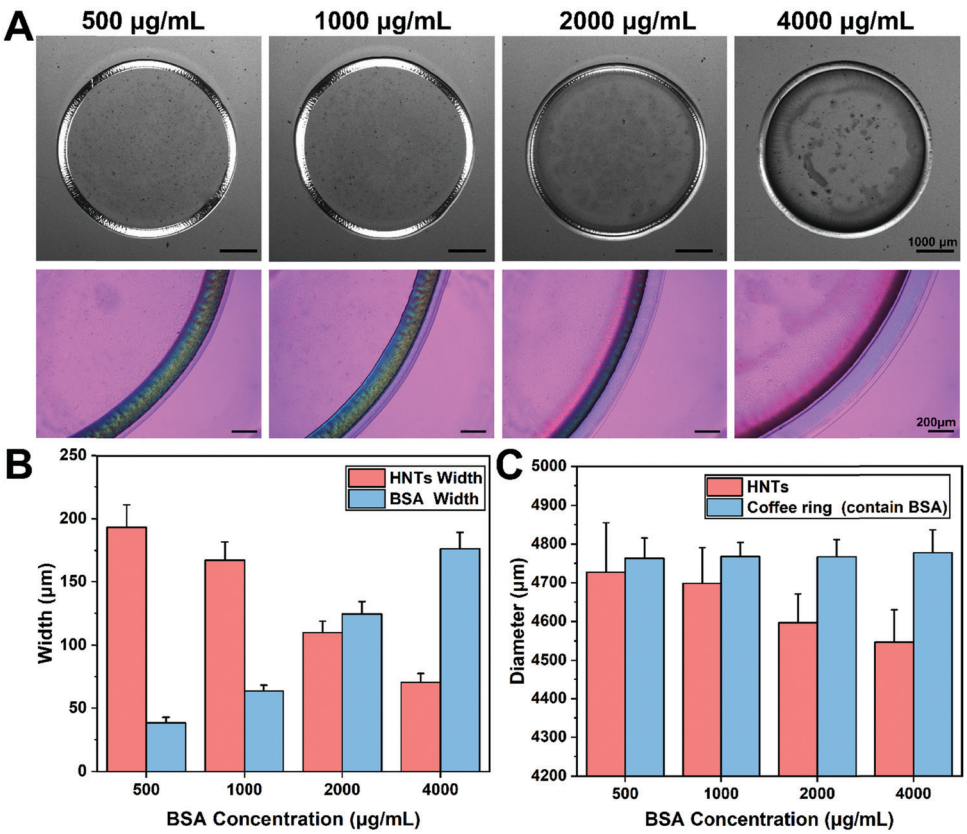

Fig. 11 Coffee-rings formed by mixtures of different concentrations BSA and HNTs: brightfield microscopy pictures and POM pictures with insertion of a 530 nm retardation plate (A); HNTs and BSA ring widths (B); whole coffee-ring and HNT ring diameters (C).

PS and PMMA, and the siliconized glass was the smallest. The evaporation time is inversely proportional to the evaporation area, and the evaporation time is directly proportional to the contact angle. So, the larger the substrate contact angle, the longer the evaporation time.

3.7. Detection of protein content by HNT coffee-ring patterns

The coffee-ring pattern can be formed by evaporating not only the dispersion of nanoparticles but also protein solutions. Proteins could also form coffee-ring patterns during droplet drying, but the formed patterns were too transparent to be detected.[5] Taking bovine serum albumin (BSA) as a representative, it was added to the HNT dispersion and the mixture was dropped on the adhesion glass slide to form a coffee-ring. Detecting the presence and concentration of BSA can be achieved by analysis of the coffee-ring pattern formed by HNTs and BSA mixture aqueous dispersion. The outer ring formed by BSA is gray-color and not obvious while the inner ring formed by HNTs could be easily distinguished by observing under a brightfield microscope. After inserting a 530 nm compensator, the approximately transparent BSA outer ring and the boundary between it and HNTs could be seen (Fig. 11A). The coffee-rings formed by the mixture of BSA and HNTs of different concentrations were prepared and characterized (Fig. 11B). It was noted that different concentrations of BSA will affect the width of the HNT ring. With the increase of BSA concentration, the ring width of HNTs gradually decreased, but the width of the coffee-ring remained at 250 μm and the diameter remained at about 4760 μm (Fig. 11C). The width and diameter of the coffee-ring formed by different contents of BSA were similar and the increase of the BSA concentration would cause the width of the HNT ring to decrease. The BSA concentration in different solutions could be compared by measuring the obvious coffee-ring and HNT ring widths. For example, different concentrations of BSA solutions (A and B) and the same concentration of HNT dispersion were mixed in equal volumes. Evaporating the mixed droplets to obtain a coffee-ring, the ring width of the visible HNT ring was measured. If the HNT ring width of A is greater than that of B, it means that the BSA concentration of A is less than that of B. This method can compare the concentration relationship of the protein contained in different solutions through simple solution mixing and evaporation. It can quantify the protein content by adding samples with different protein concentrations and measuring the coffee-ring diameters; plotting a scatter diagram between protein concentrations and ring diameter, one can describe the relationship between protein concentration and coffee-ring diameter using mathematical equations. It broadens the application of the coffee-ring in disease diagnosis, such as detection of protein content in urine.

4. Conclusions

In this study, HNT droplets were transferred into a coffee-ring pattern with an ordered structure by an evaporation-induced self-assembly method. The formation of coffee-ring patterns was studied in different ways, and a related mechanism was proposed to explain the formation of coffee-rings. The birefringence phenomenon of the coffee-ring patterns could be observed at all experimental concentrations, which indicated the existence of orderly arranged nanotubes in the ring. The ring width and height of the coffee-ring patterns increased with the increase of HNT dispersion concentration and volume. The increase of drying temperature and the addition of surfactants can enhance the Marangoni effect in the droplets and inhibit the formation of coffee-rings, so that the HNTs were evenly distributed to form a disc. By mixing the HNT dispersion with protein solutions of different concentrations to form a coffee-ring, the relationship between the protein contents in different solutions can be simply judged, which provides the possibility for the application of the HNT coffee-ring in the protein detection in disease diagnosis.

Conflicts of interest

There are no conflicts to declare.

Acknowledgements

This work was financially supported by the National Natural Science Foundation of China (52073121), the Natural Science Foundation of Guangdong Province (2019A1515011509), the Science and Technology Program of Guangzhou (202102010117), and the Fundamental Research Funds for the Central Universities (21619102).

References

1 R. D. Deegan, O. Bakajin, T. F. Dupont, G. Huber, S. R. Nagel and T. A. Witten, Capillary flow as the cause of ring stains from dried liquid drops, *Nature*, 1997, **389**(6653), 827–829.
2 R. G. Larson, Twenty years of drying droplets, *Nature*, 2017, **550**(7677), 466–467.
3 D. Mampallil and H. B. Eral, A review on suppression and utilization of the coffee-ring effect, *Adv. Colloid Interface Sci.*, 2018, **252**, 38–54.
4 D. Zang, S. Tarafdar, Y. Y. Tarasevich, M. Dutta Choudhury and T. Dutta, Evaporation of a Droplet: From physics to applications, *Phys. Rep.*, 2019, **804**, 1–56.
5 S. Devineau, M. Anyfantakis, L. Marichal, L. Kiger, M. Morel, S. Rudiuk and D. Baigl, Protein Adsorption and Reorganization on Nanoparticles Probed by the Coffee-Ring Effect: Application to Single Point Mutation Detection, *J. Am. Chem. Soc.*, 2016, **138**(36), 11623–11632.
6 S. F. Shimobayashi, M. Tsudome and T. Kurimura, Suppression of the coffee-ring effect by sugar-assisted depinning of contact line, *Sci. Rep.*, 2018, **8**(1), 17769.
7 Á. G. Marín, H. Gelderblom, D. Lohse and J. H. Snoeijer, Order-to-Disorder Transition in Ring-Shaped Colloidal Stains, *Phys. Rev. Lett.*, 2011, **107**(8), 085502.

8 I. I. Smalyukh, O. V. Zribi, J. C. Butler, O. D. Lavrentovich and G. C. L. Wong, Structure and Dynamics of Liquid Crystalline Pattern Formation in Drying Droplets of DNA, *Phys. Rev. Lett.*, 2006, **96**(17), 177801.

9 H. M. Gorr, J. M. Zueger and J. A. Barnard, Lysozyme Pattern Formation in Evaporating Drops, *Langmuir*, 2012, **28**(9), 4039–4042.

10 R. van Hameren, P. Schön, A. M. van Buul, J. Hoogboom, S. V. Lazarenko, J. W. Gerritsen, H. Engelkamp, P. C. M. Christianen, H. A. Heus, J. C. Maan, T. Rasing, S. Speller, A. E. Rowan, J. A. A. W. Elemans and R. J. M. Nolte, Macroscopic Hierarchical Surface Patterning of Porphyrin Trimers *via* Self-Assembly and Dewetting, *Science*, 2006, **314**(5804), 1433–1436.

11 C. Querner, M. D. Fischbein, P. A. Heiney and M. Drndić, Millimeter-Scale Assembly of CdSe Nanorods into Smectic Superstructures by Solvent Drying Kinetics, *Adv. Mater.*, 2008, **20**(12), 2308–2314.

12 T. Ming, X. Kou, H. Chen, T. Wang, H. L. Tam, K. W. Cheah, J. Y. Chen and J. Wang, Ordered gold nanostructure assemblies formed by droplet evaporation, *Angew. Chem., Int. Ed.*, 2008, **47**(50), 9685–9690.

13 Q. Li, Y. T. Zhu, I. A. Kinloch and A. H. Windle, Self-Organization of Carbon Nanotubes in Evaporating Droplets, *J. Phys. Chem. B*, 2006, **110**(28), 13926–13930.

14 L. Zhang, H. Liu, Y. Zhao, X. Sun, Y. Wen, Y. Guo, X. Gao, C. A. Di, G. Yu and Y. Liu, Inkjet printing high-resolution, large-area graphene patterns by coffee-ring lithography, *Adv. Mater.*, 2012, **24**(3), 436–440.

15 Z. Wang, T. Liu, Y. Yu, M. Asif, N. Xu, F. Xiao and H. Liu, Coffee Ring–Inspired Approach toward Oriented Self-Assembly of Biomimetic Murray MOFs as Sweat Biosensor, *Small*, 2018, **14**(45), 1802670.

16 M. Liu, Z. Jia, D. Jia and C. Zhou, Recent advance in research on halloysite nanotubes-polymer nanocomposite, *Prog. Polym. Sci.*, 2014, **39**(8), 1498–1525.

17 Y. Lvov, W. Wang, L. Zhang and R. Fakhrullin, Halloysite Clay Nanotubes for Loading and Sustained Release of Functional Compounds, *Adv. Mater.*, 2016, **28**(6), 1227–1250.

18 M. Liu, R. Fakhrullin, A. Novikov, A. Panchal and Y. Lvov, Tubule Nanoclay-Organic Heterostructures for Biomedical Applications, *Macromol. Biosci.*, 2019, **19**(4), 1800419.

19 X. Zhao, C. Zhou and M. Liu, Self-assembled structures of halloysite nanotubes: towards the development of high-performance biomedical materials, *J. Mater. Chem. B*, 2020, **8**(5), 838–851.

20 M. Liu, Z. Huo, T. Liu, Y. Shen, R. He and C. Zhou, Self-Assembling Halloysite Nanotubes into Concentric Ring Patterns in a Sphere-on-Flat Geometry, *Langmuir*, 2017, **33**(12), 3088–3098.

21 R. He, M. Liu, Y. Shen, Z. Long and C. Zhou, Large-area assembly of halloysite nanotubes for enhancing the capture of tumor cells, *J. Mater. Chem. B*, 2017, **5**(9), 1712–1723.

22 H. Liu, X. Cao, X. Yang, M. Liu and Y. Lvov, Formation of Regular Wormlike Patterns by Dewetting Aqueous Dispersions of Halloysite Nanotubes, *J. Phys. Chem. C*, 2020, **124**(14), 8034–8040.

23 X. Zhao, C. Zhou, Y. Lvov and M. Liu, Clay Nanotubes Aligned with Shear Forces for Mesenchymal Stem Cell Patterning, *Small*, 2019, **15**(21), 1900357.

24 Y. Zhao, G. Cavallaro and Y. Lvov, Orientation of charged clay nanotubes in evaporating droplet meniscus, *J. Colloid Interface Sci.*, 2015, **440**, 68–77.

25 C. Nobile, L. Carbone, A. Fiore, R. Cingolani, L. Manna and R. Krahne, Self-assembly of highly fluorescent semiconductor nanorods into large scale smectic liquid crystal structures by coffee stain evaporation dynamics, *J. Phys.: Condens. Matter*, 2009, **21**(26), 264013.

26 V. R. Dugyala and M. G. Basavaraj, Evaporation of Sessile Drops Containing Colloidal Rods: Coffee-Ring and Order–Disorder Transition, *J. Phys. Chem. B*, 2015, **119**(9), 3860–3867.

27 P. J. Yunker, T. Still, M. A. Lohr and A. G. Yodh, Suppression of the coffee-ring effect by shape-dependent capillary interactions, *Nature*, 2011, **476**(7360), 308–311.

28 B. Li, C. Zhang, B. Jiang, W. Han and Z. Lin, Flow-enabled self-assembly of large-scale aligned nanowires, *Angew. Chem., Int. Ed.*, 2015, **54**(14), 4250–4254.

29 B. Li, W. Han, M. Byun, L. Zhu, Q. Zou and Z. Lin, Macroscopic Highly Aligned DNA Nanowires Created by Controlled Evaporative Self-Assembly, *ACS Nano*, 2013, **7**(5), 4326–4333.

30 B. Li, W. Han, B. Jiang and Z. Lin, Crafting Threads of Diblock Copolymer Micelles via Flow-Enabled Self-Assembly, *ACS Nano*, 2014, **8**(3), 2936–2942.

31 Y. Li, C. Lv, Z. Li, D. Quere and Q. Zheng, From coffee rings to coffee eyes, *Soft Matter*, 2015, **11**(23), 4669–4673.

32 H. Lama, D. K. Satapathy and M. G. Basavaraj, Modulation of Central Depletion Zone in Evaporated Sessile Drops *via* Substrate Heating, *Langmuir*, 2020, **36**(17), 4737–4744.

33 T. Josyula, Z. Wang, A. Askounis, D. Orejon, S. Harish, Y. Takata, P. S. Mahapatra and A. Pattamatta, Evaporation kinetics of pure water drops: Thermal patterns, Marangoni flow, and interfacial temperature difference, *Phys. Rev. E*, 2018, **98**(5), 052804.

34 H. Hu and R. G. Larson, Marangoni Effect Reverses Coffee-Ring Depositions, *J. Phys. Chem. B*, 2006, **110**(14), 7090–7094.

35 M. Majumder, C. S. Rendall, J. A. Eukel, J. Y. L. Wang, N. Behabtu, C. L. Pint, T.-Y. Liu, A. W. Orbaek, F. Mirri, J. Nam, A. R. Barron, R. H. Hauge, H. K. Schmidt and M. Pasquali, Overcoming the ''Coffee-Stain'' Effect by Compositional Marangoni-Flow-Assisted Drop-Drying, *J. Phys. Chem. B*, 2012, **116**(22), 6536–6542.

Electronic Supplementary Material (ESI) for Soft Matter.

Supporting Information for

Tunable Coffee-Ring Formation of Halloysite Nanotubes by Evaporating Sessile Drops

*Hongzhong Liu, Yao Wang, Yumin Luo, Min Guo, Yue Feng, Mingxian Liu**

Department of Materials Science and Engineering, Jinan University, Guangzhou

510632, China

*Corresponding author. Email: liumx@jnu.edu.cn

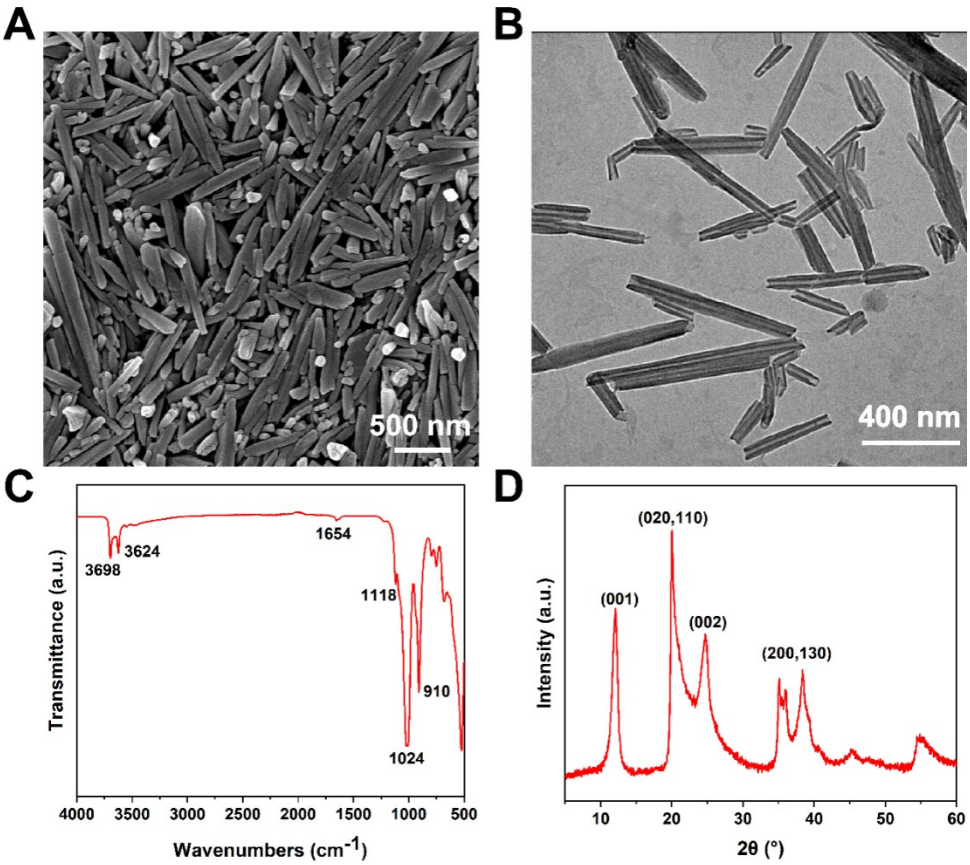

Figure S1. Characterization of halloysite nanotubes: SEM (A), TEM (B), FTIR (C) and XRD (D).

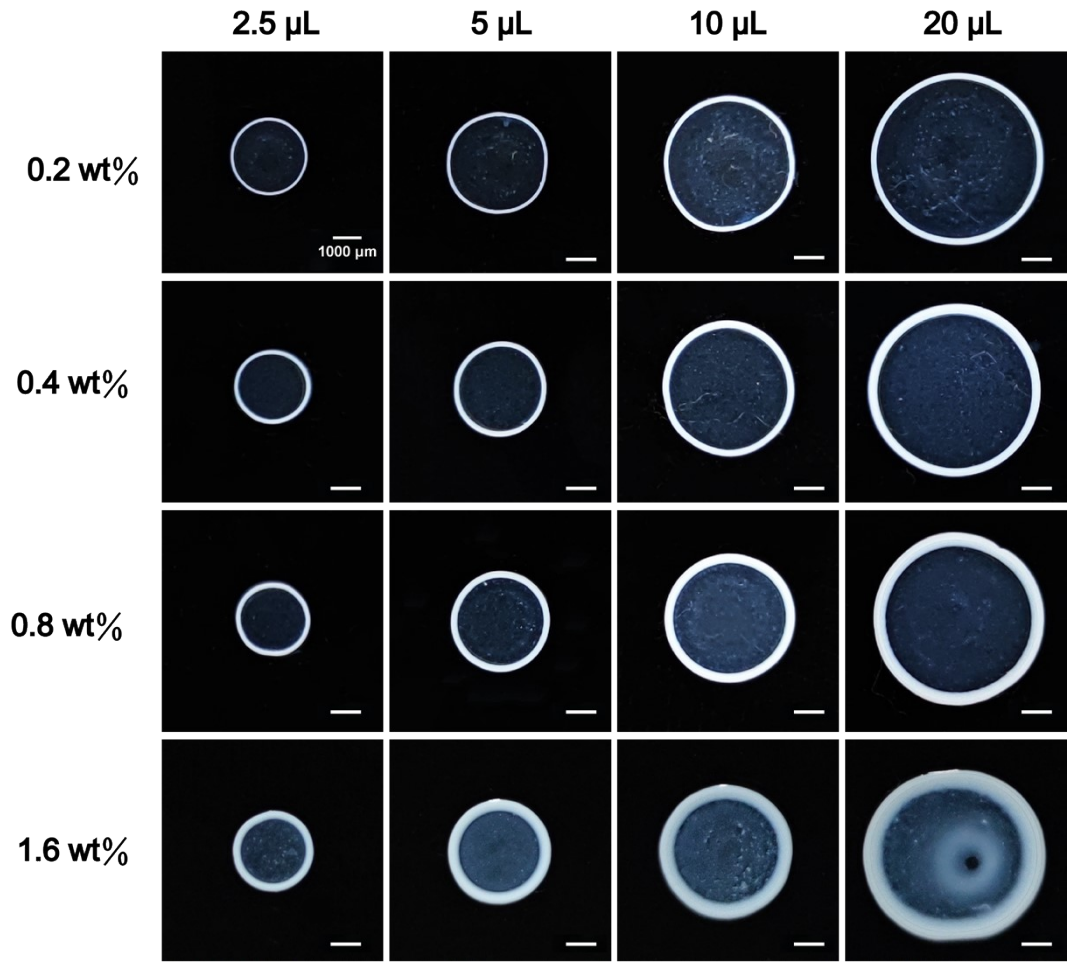

Figure S2. Appearance of HNTs coffee-ring patterns at different concentration and droplet volume.

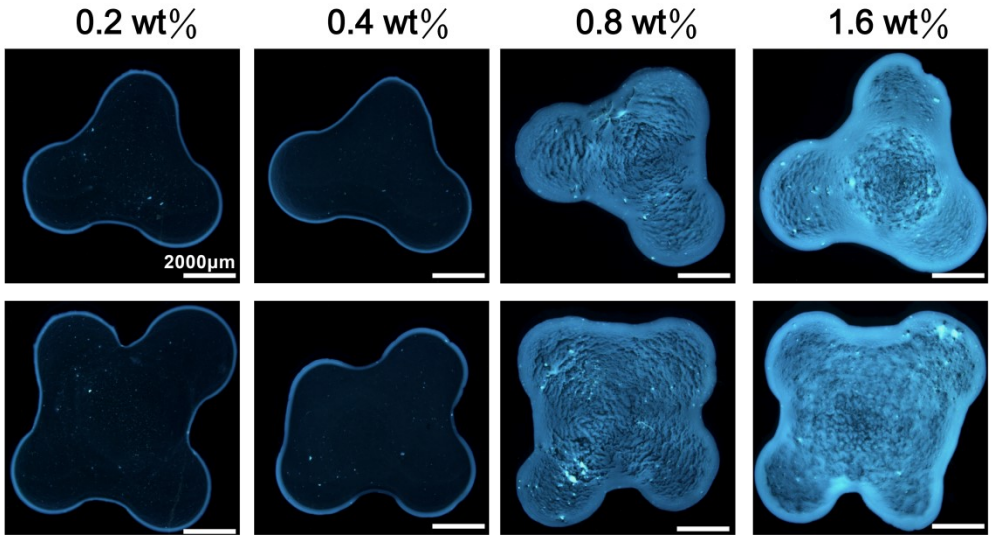

Figure S3. Different patterns formed by the interactions between three (top) and four (bottom) HNTs drops.

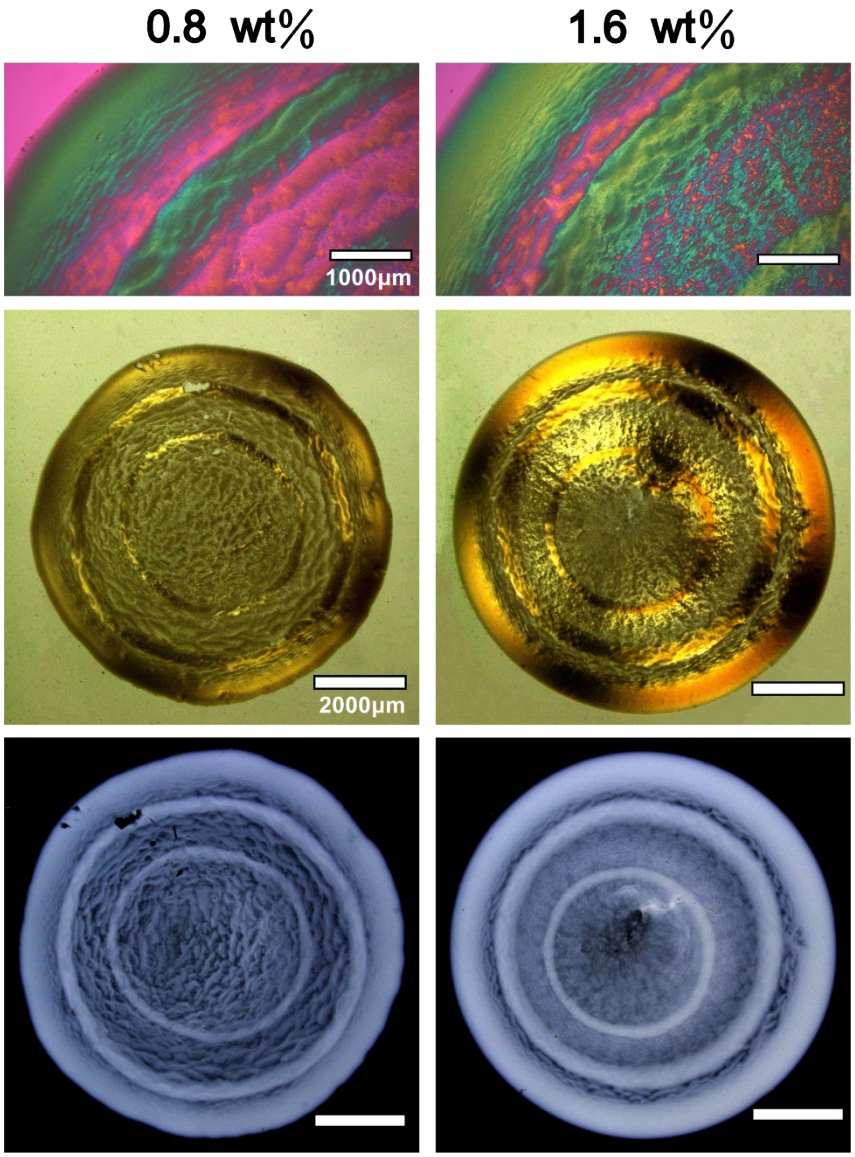

Figure S4. Ring-in-ring patterns formed by the evaporation of smaller HNTs droplet after formation of the bigger HNTs coffee-ring pattern: (A) POM images; (B) stereomicroscope images; (C) appearance photos.

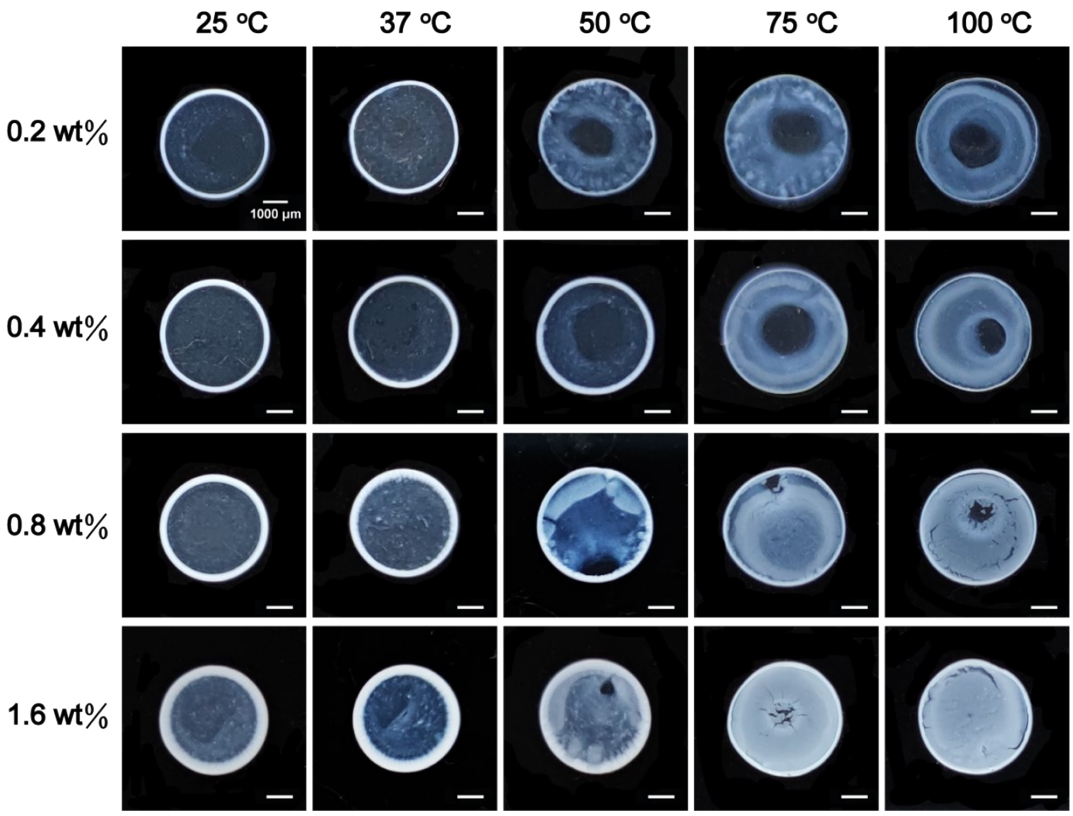

Figure S5. Effect of substrate temperature on the coffee-ring patterns at different concentration.